# Orientational relaxation in Brownian rotors with frustrated interactions on a square lattice

Sung Jong Lee[1] and Bongsoo Kim[2]
[1]*Department of Physics, The University of Suwon, Hwasung-Gun, Kyunggi-Do 445-890, Korea*
[2]*Department of Physics, Changwon National University, Changwon 641-773, Korea*
(Received 21 December 1998)

We present simulation results on the equilibrium relaxation of Brownian planar rotors based on a uniformly frustrated $XY$ model on a square lattice. The rotational relaxation exhibits typical dynamic features of fragile supercooled liquids including the two-step relaxation. We observe a dynamic crossover from the high-temperature regime with Arrhenius behavior to the low-temperature regime with temperature-dependent activation energy. A consistent picture for the observed slow dynamics can be given in terms of the caging effect and thermal activation across potential barriers in the energy landscapes. [S1063-651X(99)12608-4]

PACS number(s): 64.60.Cn, 05.45.−a, 64.70.Pf

## I. INTRODUCTION

The past decade or so has witnessed significant advances in our understanding of the underlying mechanism for the slow dynamics of supercooled liquids approaching the glass transition [1]. The development of mode-coupling theory of supercooled liquids [2] and extensive experiments and computer simulations [3] have played crucial roles in such advances. Some efforts have also been devoted to devising model systems (even though somewhat artificial) [4] which show glassy behavior similar to that of supercooled liquids. One line of research along this direction is to find (lattice) model systems with no quenched disorder but some intrinsic frustration built into the model, which may exhibit glassy relaxations [5–8].

One can imagine that there may exist a common microscopic mechanism which underlies the observed similarities in the relaxations of model systems and real supercooled liquids. This possibility is made more plausible by the universal scaling property observed in the dielectric susceptibilities of a variety of supercooled liquids [9] and some plastic (glassy) crystal [10–12]. In this work, we address the question of this possible common mechanism by investigating the equilibrium orientational relaxation of planar Brownian rotors whose interaction is prescribed by that of uniformly frustrated $XY$ (UFXY) models with dense frustration, which is a prime example of non-randomly-frustrated systems [13] characterized by complex degeneracy of ground states and many metastable states.

While a recent simulation [8] by the present authors deals with the relaxation of the vortex charge density for a purely dissipative dynamics, here we examine directly the orientational relaxation with finite rotational inertia, which offers more transparent views on the origin of the observed slow relaxation. Also, due to the one-dimensional nature of the phase of the planar rotors, it is convenient to probe the properties of the angular motions of the rotors of the system. We find that, by including phenomenological rotational inertia in the dynamic equation for the rotors, the orientational correlation exhibits a two-step relaxation, which is analogous to the (fast) $\beta$ and $\alpha$ relaxations of supercooled liquids. Mean square angular displacement (MSAD) exhibits three-stage behavior, i.e., the early time ballistic, intermediate subdiffusive, and late time diffusive regimes, which is argued to be consistent with the picture of the cage effect and long-time activated dynamics for the motion of the rotors. It is shown that there exist two dynamically distinct regimes: a high-temperature regime where the dynamics is governed by a temperature-independent activation energy, and a low-temperature regime, in which the activation energy increases with decreasing temperature, which is interpreted as arising from complex energy landscapes [14,15] probed by the system in the low-temperature regime.

## II. DYNAMIC MODEL AND SIMULATION METHOD

We consider the following Langevin dynamics for a collection of planar rotors on a square lattice,

$$I\dot{\omega}_i(t)+\gamma\omega_i(t)=-\frac{\partial V(\{\theta\})}{\partial\theta_i(t)}+\eta_i(t), \tag{1}$$

where $I$ is the moment of inertia, $\omega_i(t)\equiv\dot{\theta}_i(t)$ the angular velocity of the rotor at site $i$, $\gamma$ the damping constant, and $\eta_i(t)$ the thermal noise. Equation (1) describes the Brownian motion of rotors subject to the interaction potential energy $V(\{\theta\})$. The thermal noise $\eta_i(t)$ is given by a Gaussian random variable

$$\langle\eta_i(t)\rangle=0,$$

$$\langle\eta_i(t)\,\eta_j(t')\rangle=2\gamma T\delta_{ij}\delta(t-t'), \tag{2}$$

where the Boltzmann constant $k_B$ is set equal to unity. The variance of the noise in Eqs. (2) ensures that the system at temperature $T$ evolves toward the equilibrium state whose properties are governed by the Boltzmann distribution $\exp(-E(\{\theta\},\{\omega\})/T)$ where the energy $E(\{\theta\},\{\omega\})$ is given by $E(\{\theta\},\{\omega\})=I\Sigma_i\omega_i^2/2+V(\{\theta\})$.

Here we chose the potential energy $V(\{\theta\})$ as the energy of the two-dimensional UFXY model on a square lattice, which takes the form [16]

$$V(\{\theta\})=-J\sum_{(ij)}\cos(\theta_i-\theta_j-A_{ij}), \tag{3}$$

 

where $J$ is the coupling constant and $(ij)$ denotes nearest-neighbor pairs. The bond angles $A_{ij}$ satisfy the constraint

$$\sum_{i,j\in P} A_{ij} = 2\pi f, \tag{4}$$

where the sum is over $(i,j)$ belonging to the unit plaquette $P$ causing competing interactions (frustration) between the rotors. Here, $f$ is called the frustration parameter of the system.

A convenient choice for $A_{ij}$ is the Landau gauge which is given by $A_{ij}=0$ for every horizontal bond and $A_{ij} = \pm 2\pi f x_i$ for the vertical bond directed upward (downward) with $x_i$ being the $x$ coordinate of the site $i$. It can be readily checked that this choice of the bond angles obeys the condition (4). Due to the invariance of the Hamiltonian (1) under $f \to f+1$ and $f \to -f$, we need to consider the values of $f$ only over the range $[0,1/2]$. A physical realization of this model can be found in the two-dimensional square array of Josephson junctions under a uniform perpendicular magnetic field. In this situation, the bond angle $A_{ij}$ is identified with the line integral of the vector potential $\mathbf{A}$ of the transverse magnetic field: $A_{ij} = (2\pi/\Phi_0)\int_i^j \mathbf{A}\cdot d\mathbf{l}$, where $\Phi_0$ is the flux quantum $\Phi_0 \equiv hc/2e$ per unit plaquette. With this identification the strength of magnetic field $B$ is given by $Ba^2 = f\Phi_0$, where $a$ is the lattice constant.

The UFXY model can be mapped [17] onto that of a lattice Coulomb gas with charges of magnitude $(n-f)$, $n = 0, \pm 1, \pm 2, \ldots$, where charges correspond to phase vortices with suitably defined vorticity around the plaquettes. The lowest excitation consists of charges with magnitudes $1-f$ and $-f$, respectively. The charge neutrality condition then implies that the number density of positive charges is equal to $f$. For the case of $f=0$, the well-known Kosterlitz-Thouless transition [18] occurs via vortex-antivortex unbinding at a finite temperature. Except for this case of the unfrustrated $XY$ model, the equilibrium nature and associated phase transitions of these systems are not very well understood even for the next simplest case of $f=\frac{1}{2}$, the so-called full frustrated $XY$ model [19]. For example, the ground-state configurations for the case of general $f=p/q$ ($p$ and $q$ are relative primes) are not known [20,21] except for some low-order rational values of $f$, such as $f=\frac{1}{2}, \frac{1}{3}, \frac{2}{5}, \frac{3}{8}$, etc., where staircase types of ground-state configurations are known analytically [22,21].

As $q$ becomes large (the limit of irrational frustration), due to the complexity of the degeneracy of the system and long equilibration time, it is quite a difficult task to analyze the nature of the low-temperature phase of the system. And, in spite of the recent claim by Denniston and Tang [23] that there exists a first-order transition near $T_c \simeq 0.13J$, in the case of $f=1-g$ [$g$ being the golden-mean ratio $g=(\sqrt{5}-1)/2 \simeq 0.618$] it is fair to say that the low-temperature phase is not completely understood yet. On the other hand, since it is clear that many metastable states are possible due to the dense frustration, one can expect that Brownian dynamics (1) with the potential energy (3) may generate a slow relaxation, where trapping of the configurations in deep metastable minima and thermal activation across the potential barriers play a crucial role. Note that there is no intrinsic disorder in the present system, which distinguishes itself from a spin glass system where both intrinsic disorder and frustration are considered to be essential [24].

With the potential energy (3), the Langevin equation is explicitly given by

$$I\dot{\omega}_i(t) + \gamma\omega_i(t) = -J\sum_j \sin(\theta_i - \theta_j - A_{ij}) + \eta_i(t). \tag{5}$$

We integrate Eq. (5) in time, starting from random initial conditions $\{\theta_i(0)\}$ and $\{\omega_i(0)\}$ using an Euler algorithm on a square lattice of linear size $N=34$. In our simulations, we used $I=1.5$, $\gamma=1$, $J=1$, and $f=13/34$, which is a Fibonacci approximant to $f=1-g$. Periodic boundary conditions are employed for both spatial directions. The results were averaged over 150~1000 different random initial configurations, depending on the quenching temperature. As for the integration time step, we used $dt=0.05$ in the dimensionless unit of time. No essential difference could be found in the results when compared with those obtained by using $dt=0.01$.

## III. RESULTS AND DISCUSSIONS

In order to probe the orientational relaxation of the system, we first computed the on-site autocorrelation function for the planar spins

$$C_R(t) = \frac{1}{N^2}\left\langle \sum_{i=1}^{N^2} \cos[\theta_i(0) - \theta_i(t)] \right\rangle, \tag{6}$$

where the bracket $\langle \cdots \rangle$ in Eq. (6) represents an average over different random initial configurations. In this work we focus only on the lowest-order correlation even though one may also measure the higher-order correlations, as was done in recent molecular-dynamics simulations [25–27].

Shown in Fig. 1 is the on-site autocorrelation function $C_R(t)$. The relaxation continuously slows down as the temperature is lowered. In order to characterize the slowing down of the relaxation, one can define a characteristic relaxation time $\tau_R(T)$ as $C_R(\tau_R) = 1/e$. The temperature dependence of $\tau_R(T)$ is shown in the inset of Fig. 1. It exhibits an Arrhenius behavior at high temperatures, while at low temperatures ($T<0.20$) it shows a non-Arrhenius behavior, which can be well fitted by the Vogel-Tamman-Fulcher form $\tau_R(T) = \tau_0 \exp[DT_0/(T-T_0)]$ with $\tau_0 \simeq 9.92$, $T_0 \simeq 0.08$, and $D \simeq 3.58$ [28]. Similar non-Arrhenius behavior was observed in the vorticity relaxation as well [8].

An interesting feature of the rotational relaxation is that it exhibits a two-step relaxation, a very fast relaxation (up to $t \simeq 3$ for $T=0.13J$, the lowest temperature probed), and a slow relaxation following the fast relaxation. The earliest part of the fast relaxation is expected to be well described by the free rotation of the rotors $I\dot{\omega}_i(t) + \gamma\omega_i(t) = 0$. For the time range where $t \ll I$, the inertial term is dominant and hence $\theta_i(t) - \theta_i(0) \simeq \omega_i(0)t$. It is then easy to show that the relaxation is given by $C_R(t) \simeq 1 - (T/2I)t^2$ using the equipartition theorem $\langle \omega^2 \rangle = T/I$.

The long-time part of the slow relaxation can be well fitted by the stretched exponential form $C_R(t) = C_0 \exp[-C_1(t/\tau_R)^\beta]$ ($C_1 = 1 + \ln C_0$ due to the definition of $\tau_R$), shown in Fig. 2. We find that the exponent $\beta$ varies with

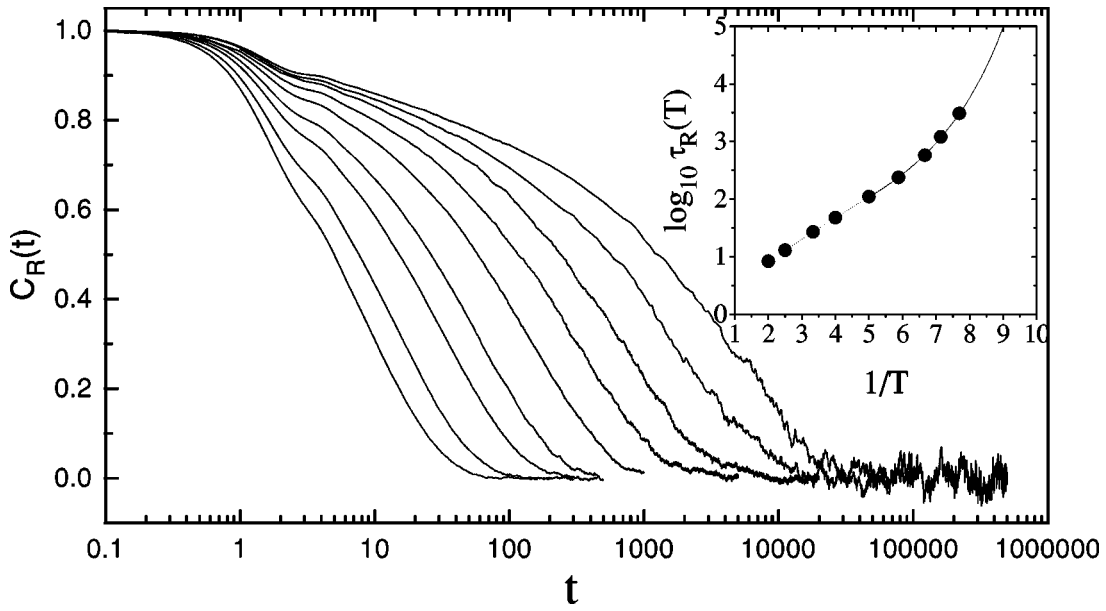


FIG. 1. The rotational autocorrelation functions $C_R(t)$ versus time $t$ (in dimensionless units with $\gamma=1$ and $J=1$) for temperatures $T/J=0.5$, 0.4, 0.3, 0.25, 0.2, 0.17, 0.15, 0.14, 0.13. Inset: An Arrhenius plot for the characteristic relaxation time defined as $C(\tau_R(T)) \equiv 1/e$, where the solid line is a Vogel-Tamman-Fulcher fit at the low-temperature regime (see the text).

temperature: it decreases as the temperature is lowered, as shown below in the inset of Fig. 3. It is interesting to note that at low temperatures ($T \leqslant 0.2$) the short-time part of the slow relaxation shows a deviation from its stretched exponential fit and the time region for this deviation tends to extend over longer time regions with lowering temperature. We have fitted this region with a power-law decay known as the von-Schweider relaxation [29] $C_R(t)=C_2-C_3t^b$, where the exponent $b$ also varies with temperature (see the inset of Fig. 3). We now examine the scaling behavior of the rotational relaxation. Shown in Fig. 3 is $C_R(t)$ versus the rescaled time $t/\tau_R(T)$. Obviously the earliest part of the relaxation does not obey the scaling since a faster time scale (the inverse of the inertia which is temperature independent) is involved in this regime. We also observe that the time-temperature superposition of the relaxation function is systematically violated in the late (slow) part of the relaxation, especially at low temperatures. This breakdown of the scaling is consistent with the fact that the two exponents $b$ and $\beta$ vary with temperature.

It would be interesting to examine the response function corresponding to the orientational correlation function $C_R(t)$. The response function in the frequency ($\nu$) domain can be defined as (via the fluctuation dissipation theorem) $\chi''(\nu)=2\pi\nu\int_0^\infty dt \cos(2\pi\nu t)C_R(t)$. Figure 4 shows $\chi''(\nu)$ versus $\nu$ in a semilogarithmic plot. We see that there exist two peaks, the low-frequency $\alpha$ peak and the high-frequency peak (microscopic peak). As the temperature is lowered, the $\alpha$ peak moves to lower frequency, indicating the slowing down of the reorientational relaxation. At the same time, the

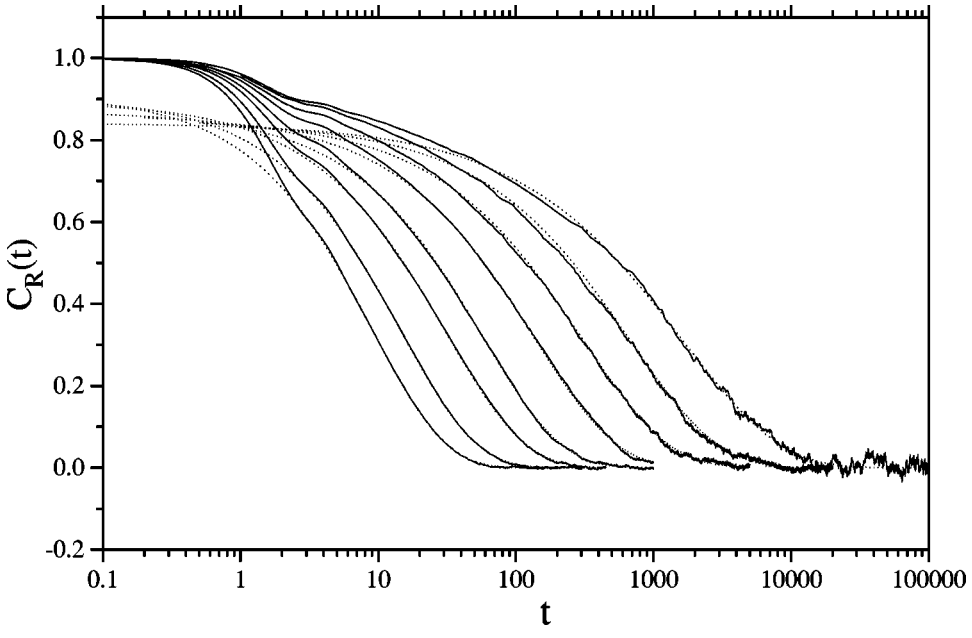


FIG. 2. Stretched exponential fit (dashed lines) to the long time part of the autocorrelation functions (for the same temperatures as in Fig. 1). Time $t$ is measured in the same dimensionless units as in Fig. 1.

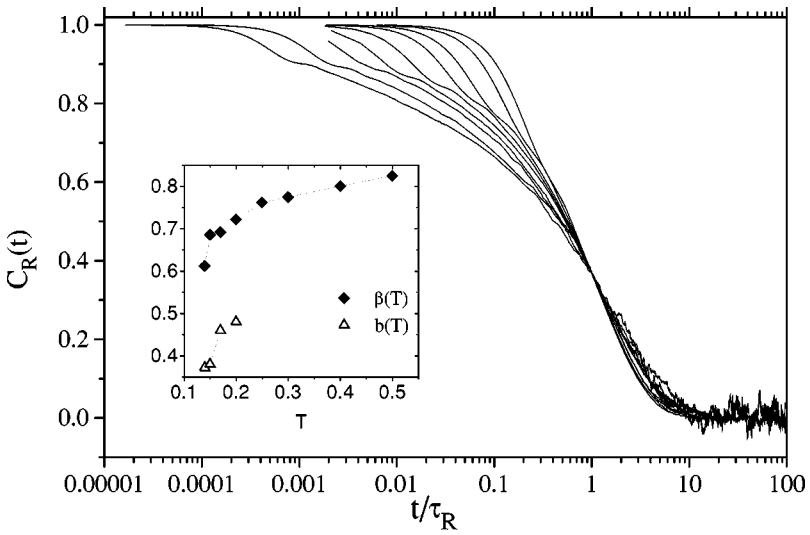


FIG. 3. Rotational autocorrelation functions $C_R(t)$ versus the rescaled time $t/\tau_R(T)$. Note that the time-temperature superposition is systematically violated. The inset shows the temperature dependence of the exponents $b(T)$ and $\beta(T)$ characterizing the slow part of the correlation function $C_R(t)$.

maximum value of $\chi''(\nu)$, which is analogous to the Debye-Waller factor, continuously decreases, and the $\alpha$ spectrum becomes broadened as the temperature is lowered. We also note that as the temperature is lowered, a minimum of the spectrum is slowly developed. All these features in the frequency spectrum of the orientational relaxation are qualitatively quite similar to the recent broad band dielectric susceptibility measurement of supercooled liquids [9,30,31]. According to the recent dielectric susceptibility data, the $\alpha$ spectrum of supercooled liquids consists of two power law regimes in the right-hand side of the $\alpha$ peak. The first power-law relaxation clearly corresponds to the stretched exponential relaxation in time domain. In addition to this, another power law regime is observed in the high-frequency side of the $\alpha$ spectrum. It is quite interesting that similar power-law relaxation is also observed in the high-frequency part of the magnetic susceptibility of a spin glass system [32]. Although we cannot better resolve the high-frequency part of the $\alpha$ spectrum of the present orientational relaxation due to the bad statistics of the spectrum at low temperatures, we believe that our orientational relaxation spectrum also exhibits similar two-power-law regimes in the right-hand side of the $\alpha$ peak. The reason is that, even though the long-time part of $C_R(t)$ can be well fitted by a stretched exponential function, the regime of its validity (for the stretched exponential form) is limited to the late-time regime only and does not extend to the intermediate time regime where so-called von-Schweidler relaxation [33] (with different exponent $b$) better fits the relaxation function. In the frequency domain this will correspond to two-power-law behavior.

In order to investigate the self-diffusion of the rotors, we measured the mean squared angular displacement (MSAD)

$$\langle[\Delta\theta(t)]^2\rangle = \frac{1}{N}\left\langle \sum_{i=1}^{N} [\theta_i(t)-\theta_i(0)]^2 \right\rangle, \tag{7}$$

where the phase angle $\theta_i(t)$ is unbounded. Figure 5 shows a log-log plot for the MSAD $\langle[\Delta\theta(t)]^2\rangle$ versus time $t$. For all temperature ranges probed, we see that $\langle[\Delta\theta(t)]^2\rangle \sim t^2$ in the early time regime, which may be called the ballistic regime. It is expected that each rotor makes a free rotation in this time regime. Hence the MSAD is then given by $\langle[\Delta\theta(t)]^2\rangle \simeq (T/I)t^2$ in the ballistic regime. This regime corresponds to the earliest part of the relaxation $C_R(t) \simeq 1 - (T/2I)t^2$. For high temperatures this ballistic regime di-

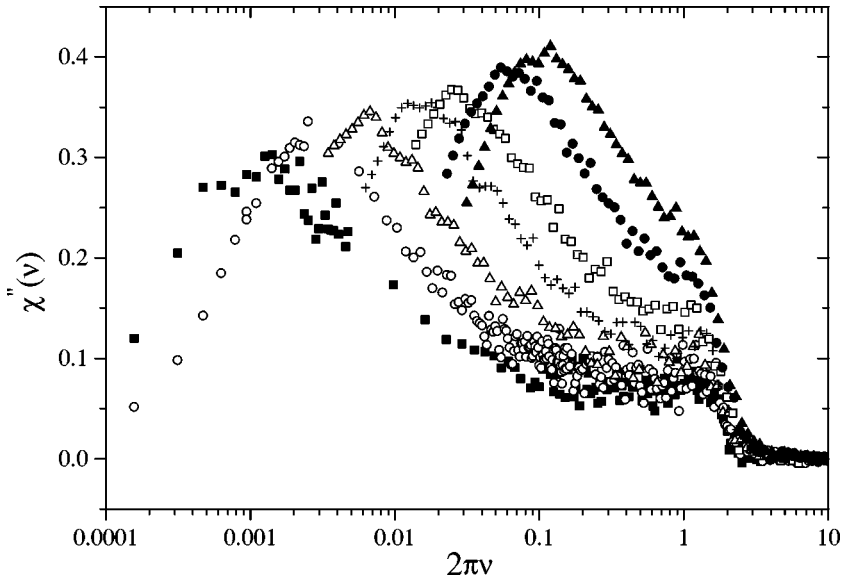


FIG. 4. Dynamic response function $\chi''(\nu)$ corresponding to the rotational relaxation versus frequency $\nu$ for temperatures $T=0.5$, 0.4, 0.3, 0.25, 0.2, 0.17, 0.15. In addition to the microscopic peak, one can clearly see the development of the $\beta$ minimum (as the temperature is lowered), a decrease of the height of the $\alpha$ peak, and a broadening of the width of the $\alpha$ peak.

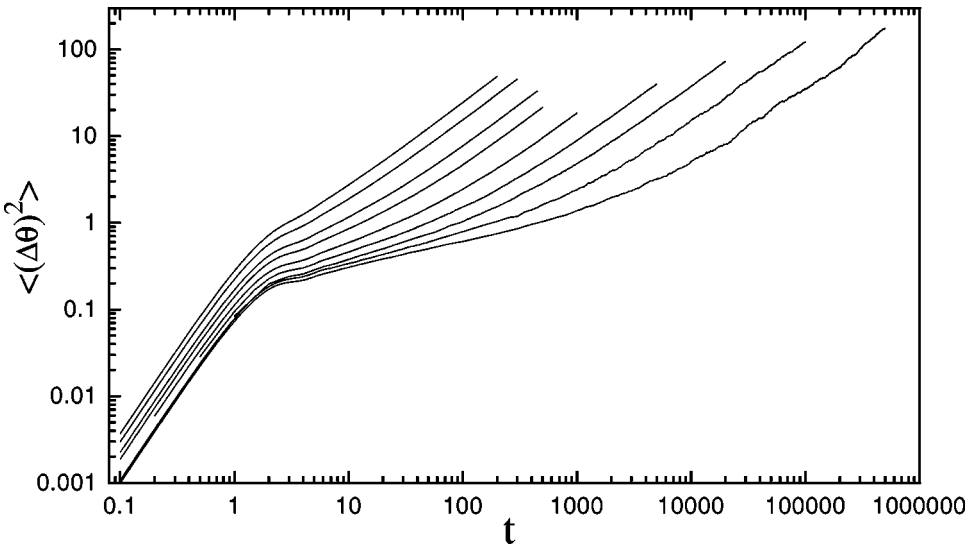


FIG. 5. Mean squared angular displacement $\langle[\Delta\theta(t)]^2\rangle$ versus time $t$ (in dimensionless units) for the same temperatures as in Fig. 1. At the lowest temperature probed ($T=0.13J$), the subdiffusive regime extends over more than two decades.

rectly crosses over to the diffusive regime where $\langle[\Delta\theta(t)]^2\rangle\sim t$. But as the temperature is lowered, in the intermediate time regime a subdiffusive regime characterized by $\langle[\Delta\theta(t)]^2\rangle\sim t^{\phi}$ with $\phi<1$ (for example, $\phi\simeq 0.3$ for $T=0.13J$) starts to appear and extends over more than two decades of time at the lowest temperature probed ($T=0.13J$). The subdiffusive regime sets in at the same time $t\approx 2$ for all temperatures. In this regime the rotational motion is significantly hindered. This can be directly seen in Fig. 6, which shows the angular displacements $\Delta\theta_i(t)\equiv\theta_i(t)-\theta_i(0)$ at some representative sites at $T=0.15J$. We clearly see from this figure that for all these phase angles the rotational motion looks almost frozen for more than a few thousand time units. This strongly indicates that the system is stuck in a particular configuration among many possible metastable states. The rotor then executes a local vibrational motion only, which corresponds to the caging in the dynamics of real supercooled liquids. At longer time scales, however, the local rotors can execute full rotations via activated tunneling through the potential barriers, showing occasional abrupt rotational motions, as shown in Fig. 6. Similar jump motions have been observed in MD simulations of soft-sphere mixtures [34], binary Lennard-Jones [35], and the colloidal glass [36]. Also, neighboring rotors can execute collective rotations, thereby slowly rearranging the whole phase configurations. This stage will correspond to the slow part of $C_R(t)$. This entire time evolution of the self-rotational motion is qualtitatively the same as that observed in MD simulations of the orientational relaxation of molecular supercooled liquids [27].

The rotational diffusion constant $D_R(T)$ can be obtained by the slope of the MSAD versus $t$ in the long-time limit where MSAD exhibits diffusive behavior $\langle[\Delta\theta(t)]^2\rangle=2D_R(T)t$. As shown in Fig. 7, at high temperatures the rotational diffusion constant exhibits an Arrhenius behavior, which is well fitted by $D_R(T)=D_0\exp(-\Delta E/T)$ with $D_0$

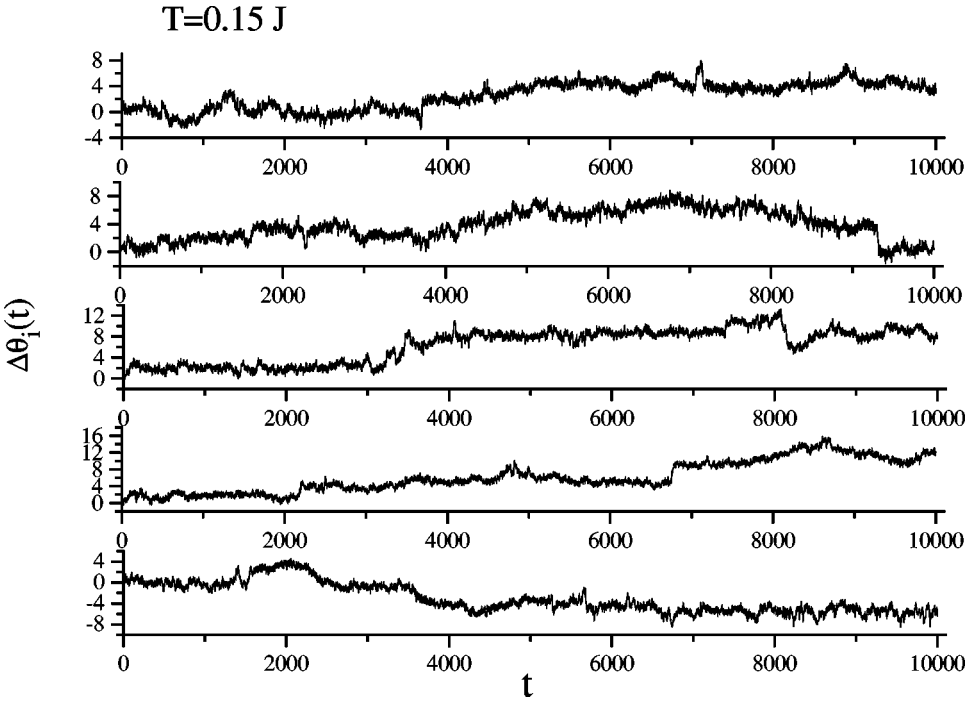


FIG. 6. Angular displacement $\Delta\theta_i(t)$ versus time $t$ (in dimensionless units) at some chosen lattice sites for $T=0.15J$. Rotational caging effect and occasional jump motions is exhibited.

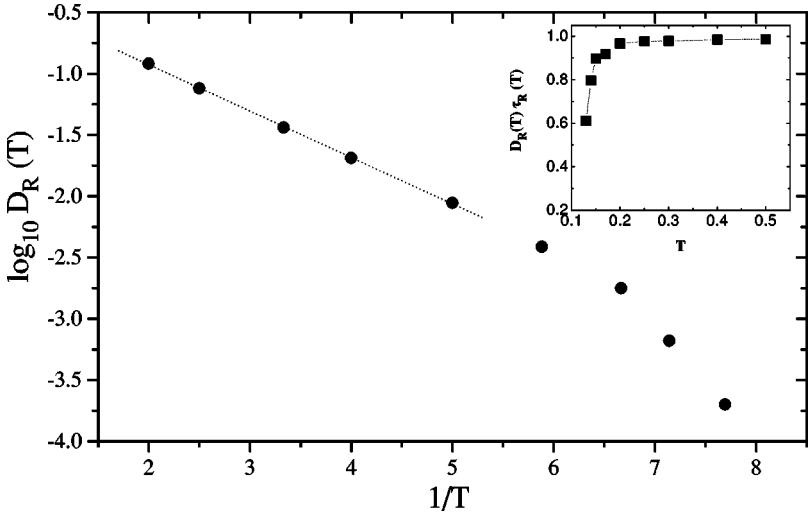


FIG. 7. An Arrhenius plot for the rotational diffusion constant $D_R(T)$. We can see a crossover from the high-temperature regime with Arrhenius behavior to the low-temperature regime with non-Arrhenius behavior. The inset shows an anomalous deviation from the Stokes-Einstein relation by plotting the product $D_R(T)\tau_R(T)$ versus $T$, where we can find that, at low temperaures, the coefficient of angular diffusion is smaller than that which would be expected from the standard Stokes-Einstein relation.

$\simeq 0.68$ and the temperature-independent activation energy $\Delta E \simeq 0.87J$. As the temperature is lowered, however, $D_R(T)$ shows a strong deviation from the Arrhenius behavior. This behavior implies that the long-time dynamics in the high-temperature regime is governed by activation barriers whose average height does not depend on temperature. In the low-temperature regime, the rotors explore deeper valleys in the potential energy landscapes whose depth increases as the temperature decreases, giving rise to the non-Arrhenius behavior of the relaxation time [37].

It was observed in some experiments of supercooled liquids [38] that while both translational and rotational diffusion constants are proportional to the inverse of viscosity at high temperatures, the decrease of the translational diffusion constant is less dramatic than the inverse of viscosity at low temperatures. The rotational diffusion constant, on the other hand, is still proportional to the inverse of viscosity at low temperatures down to the glass transition. This relative enhancement of the translational self-diffusion is also revealed in recent simulations of supercooled liquids [39,40] and the lattice model systems [41,42]. Here we compared the temperature dependences of the two time scales $1/D_R(T)$ and $\tau_R(T)$. Shown in the inset of Fig. 7 is a plot for $D_R(T)\tau_R(T)$ versus $T$. Since the product $D_R(T)\tau_R(T)$ in the plot is measured to be nearly contant down to $T=0.20J$, the two time scales are observed to be proportional to each other, i.e., $\tau_R(T) \sim D_R(T)^{-1}$ up to $T=0.20J$. The data points below $0.20J$ tend to deviate from this proportionality, indicating more rapid decrease (rather than enhancement) of the rotational diffusion constant. However, it is not clear to us whether this anomalous behavior is a genuine feature of the present model or not.

We have also measured the normalized angular velocity autocorrelation function (AVCF)

$$C_{\mathrm{AV}}(t) = \frac{\left\langle \sum_{i=1}^{N^2} \omega_i(0)\,\omega_i(t) \right\rangle}{\left\langle \sum_{i=1}^{N^2} \omega_i^2(0) \right\rangle}. \tag{8}$$

In the absence of the interaction between rotors, $C_{\mathrm{AV}}(t)$ can be easily obtained as $C_{AV}(t) = \exp(-\gamma t/I)$. With interaction, as shown in Fig. 8, the AVCF shows a strongly damped oscillatory motion. As the temperature is lowered, the amplitude of oscillation becomes enhanced. This behavior strongly indicates that the rotors execute angular rattlings in ''cages'' [43].

For purely Gaussian distribution of the angular displacements, it is easy to show that the rotational correlation function $C_R(t)$ can be expressed in terms of the mean square

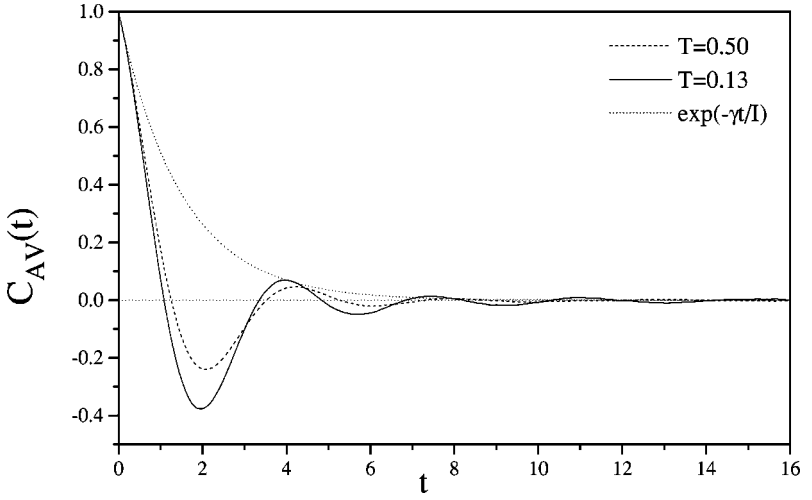


FIG. 8. The angular velocity autocorrelation functions $C_{\mathrm{AV}}(t)$ for $T=0.50J$ and $T=0.13J$ ($t$ in dimensionless units). For comparison, the dotted line represents exponential relaxation corresponding to the situation where the potentials are neglected. One can see a strong rotational cage effect indicated by the oscillating tail of $C_{\mathrm{AV}}(t)$.

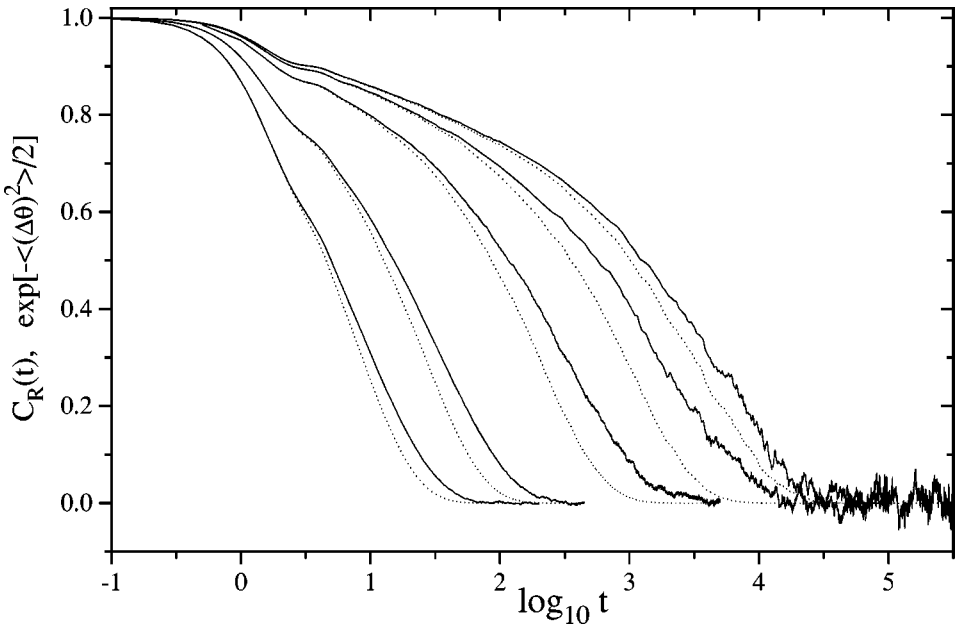


FIG. 9. The rotational autocorrelation functions versus time $t$ (in dimensionless units) for temperatures $T/J=0.5$, 0.3, 0.17, 0.14, and 0.13 together with Gaussian approximation results (dotted lines). Systematic deviations are seen at a late time stage.

angular displacement $\langle[\Delta\theta(t)]^2\rangle$ as $C_R^{(G)}(t) \equiv \exp(-\langle[\Delta\theta(t)]^2\rangle/2)$. Shown in Fig. 9 is the comparison of the rotational correlation function $C_R(t)$ and its Gaussian approximation $C_R^{(G)}(t)$. We find that $C_R(t)$ exhibits a good agreement with the Gaussian approximation in the early time regime, whereas it shows a considerable deviation from the Gaussian approximation in the late time regime. In order to characterize the non-Gaussian nature of the distribution of displacements, the non-Gaussian parameter has often been used in simulations of supercooled liquids [44–47]. Here we measure the same quantity for the angular displacements, which is defined as

$$\alpha_2(t)=\frac{1}{3}\frac{\langle[\Delta\theta(t)]^4\rangle}{\langle[\Delta\theta(t)]^2\rangle^2}-1, \tag{9}$$

where the factor $\frac{1}{3}$ comes from the one-dimensional nature for the motion of the rotors. As shown in Fig. 10, $\alpha_2(t)$ exhibits three time regimes of distinct behavior, as in the MSAD. It almost vanishes in the ballistic regime and then rapidly increases toward its maximum in the intermediate time regime, and finally decreases again in the long time regime. This temporal behavior is qualitatively the same as that observed in some MD simulations [46].

As the temperature is lowered, the maximum value of $\alpha_2(t)$ rapidly increases, and at the same time the time regime where $\alpha_2(t)$ increases is extended, indicating the strong non-Gaussian nature of the rotational motion in this regime. This regime corresponds to the subdiffusive regime in the time dependence of the MSAD shown in Fig. 5. It is expected that $\alpha_2(t)$ eventually decays to zero since, for pure diffusion, the Gaussian distribution is expected for the angular displacement.

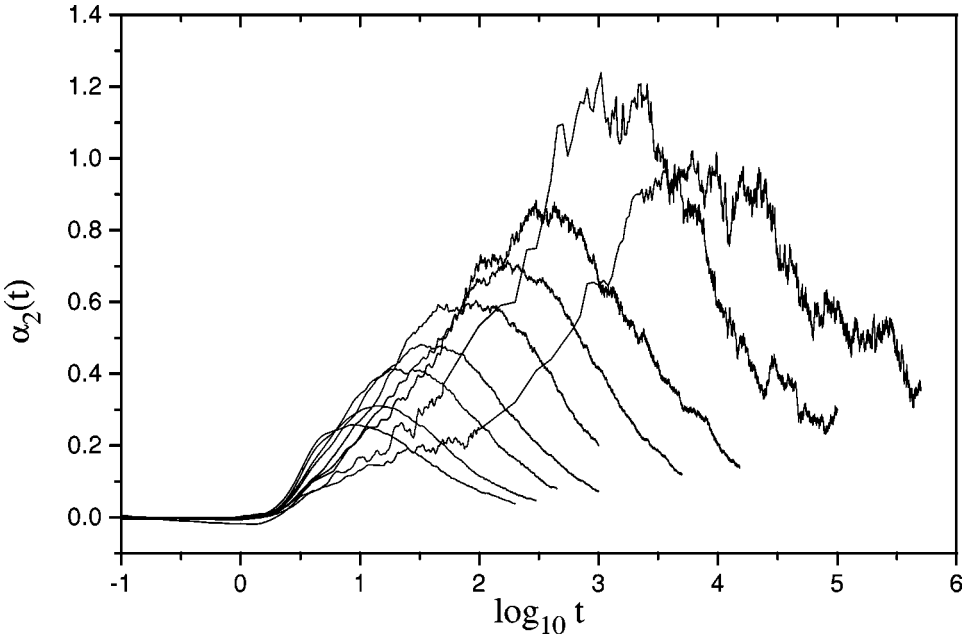


FIG. 10. Non-Gaussian parameter versus time $t$ (in dimensionless units) for the same temperatures as in Fig. 1.

## IV. SUMMARY

We have shown that the relaxation of phenomenological Brownian rotors based on the densely frustrated *XY* model Hamiltonian exhibits a slow dynamics which is remarkably similar to the relaxation of fragile supercooled liquids. We find that there exists a dynamic crossover from the high-temperature regime, where the dynamics can be described by temperature-independent activation energy, and the low-temperature regime, where non-Arrhenius behavior sets in, which can be attributed to the dynamic characteristics of the system probing deeper valleys in the potential energy landscapes with increasing height of the activation energy barrier. The caging in the metastable minima and thermal activation across potential barriers in the energy landscapes may provide the underlying physical origin for the similarity in the slow dynamic behavior of the present model system and that of real fragile supercooled liquids. It would be very interesting to quantitatively characterize the metastable states present in the system such as finding the local minima and densities of metastable states. In this regard, it would also be very instructive to examine how the dynamic features change as the value of the frustration parameter *f* is varied. We can also consider the Newtonian dynamics version of our system and compare with Langevin dynamics [48,49], which may provide further insight into these questions. We will undertake further study along these directions in the near future.

## ACKNOWLEDGMENTS

We thank Kyozi Kawasaki, Sidney Nagel, and Peter Lunkenheimer for valuable discussions. This work was supported by BSRI (BSRI 98-2412) and by SERI, Korea, through CRAY R&D 98. We also acknowledge the generous allocation of computing time from the Supercomputing Center at Tong-Myung Institute of Technology.

[1] For recent reviews, see (a) articles in the frontiers of material science in Science **267**, 1615 (1995); (b) M. D. Ediger, C. A. Angell, and S. R. Nagel, J. Phys. Chem. **100**, 13 200 (1996).

[2] The mode coupling theory of supercooled liquids is reviewed in (a) B. Kim and G. F. Mazenko, Adv. Chem. Phys. **78**, 129 (1990); (b) W. Gdotze and L. Sjögren, Rep. Prog. Phys. **55**, 241 (1992); (c) R. Schilling, in *Disordered Effects on Relaxational Processes*, edited by R. Richert and A. Blumen (Springer-Verlag, Berlin, 1994); (d) *Special Issue Devoted to Relaxation Kinetics in Supercooled Liquids-Mode Coupling Theory and Its Experimental Tests*, edited by S. Yip, Transp. Theory Stat. Phys. **24** (1995); (e) K. Kawasaki, in *Progress in Statistical Physics*, Proceedings of the International Conference in Statistical Physics in Memory of Professor Soon-Tahk Choh, edited by W. Sung *et al.* (World Scientific, Singapore, 1998).

[3] Prog. Theor. Phys. Suppl. **126** (1997), *Dynamics of Glass Transition and Related Topics*, Proceedings of Yukawa International Seminar.

[4] Model glassy systems may be categorized into two classes. The first class includes models which have a trivial Hamiltonian. The glassy behavior in this class of models is due to kinetic constraints present in the models. Facilitated kinetic Ising models [G. H. Fredrickson and H. C. Andersen, Phys. Rev. Lett. **53**, 1244 (1984)], lattice-gas models with constraint [W. Kob and H. C. Andersen, Phys. Rev. E **48**, 4364 (1993)], and the rotating hard needle model [C. Renner, H. Löwen, and J. L. Barrat, *ibid.* **52**, 5091 (1995)] belong to this class. See J. Jäckle, Prog. Theor. Phys. Suppl. **126**, 53 (1997), for further discussions on the dynamics of this class of model systems. The second class of models are characterized by their nontrivial random or/and frustrated Hamiltonians, which give rise to glassy behavior. Potts glass, *p*-spin-interaction spin glass models [J. P. Bouchaud, L. Cugliandolo, J. Kurchan, and M. Mézard, Physica A **222**, 243 (1996), and references therein], and the frustrated lattice gas model [M. Nicodemi and A. Coniglio, Phys. Rev. E **57**, R39 (1998)], as well as the present model belong to this class. The nature of the possible relationship between these two classes is an important question to be resolved.

[5] J. P. Bouchaud and M. Mézard, J. Phys. I **4**, 1109 (1994); see also J. P. Bouchaud, L. F. Cugliandolo, J. Kurchan, and M. Mézard, in *Spin Glasses and Random Fields*, edited by A. P. Young (World Scientific, Singapore, 1998).

[6] S. Franz and J. Hertz, Phys. Rev. Lett. **74**, 2114 (1995).

[7] P. Chandra, L. B. Ioffe, and D. Sherrington, Phys. Rev. Lett. **75**, 713 (1995); P. Chandra, M. V. Feigelman, and L. B. Ioffe, *ibid.* **76**, 4805 (1996); P. Chandra, M. V. Feigelman, L. B. Ioffe, and D. M. Kagan, Phys. Rev. B **56**, 11 553 (1997); P. Chandra, L. B. Ioffe, and D. Sherrington, *ibid.* **58**, R14 669 (1998).

[8] B. Kim and S. J. Lee, Phys. Rev. Lett. **78**, 3709 (1997).

[9] P. K. Dixon, L. Wu, S. R. Nagel, B. D. Williams, and J. P. Carini, Phys. Rev. Lett. **65**, 1108 (1990). See also for criticisms and discussions on this, A. Kudlik *et al.*, Europhys. Lett. **32**, 511 (1995); S.R. Nagel *et al.*, *ibid.* **36**, 473 (1996); A. Kudlik *et al.*, *ibid.* **36**, 475 (1996).

[10] H. Suga, in *Slow Dynamics in Condensed Matter*, Proceedings of The First Tohwa International Symposium (American Institute of Physics, New York, 1991).

[11] D. L. Leslie-Pelecky and N. O. Birge, Phys. Rev. Lett. **72**, 1232 (1994); Phys. Rev. B **50**, 13 250 (1994).

[12] R. Brand, P. Lunkenheimer, and A. Loidl, Phys. Rev. B **56**, R5713 (1997).

[13] D. R. Nelson, Phys. Rev. B **28**, 5515 (1983); D. R. Nelson, in *Application of Field Theory to Statistical Mechanics*, edited by L. Garrido (Springer-Verlag, New York, 1984).

[14] M. Goldstein, J. Chem. Phys. **51**, 3728 (1969).

[15] F. Stillinger, Science **267**, 1939 (1995).

[16] S. Teitel and C. Jayaprakash, Phys. Rev. B **27**, 598 (1983).

[17] J. Villain, J. Phys. (Paris) **36**, 581 (1975); J. V. José, L. P. Kadanoff, S. Kirkpatrick, and D. R. Nelson, Phys. Rev. B **16**, 1217 (1977).

[18] J. M. Kosterlitz and D. Thouless, J. Phys. C **6**, 1181 (1973); J. M. Kosterlitz, *ibid.* **7**, 1046 (1974).

[19] For a review, see E. Granato, J. M. Kosterlitz, and M. P. Nightingale, Physica B **222**, 266 (1996).

[20] T. C. Halsey, Phys. Rev. Lett. **55**, 1018 (1985); Physica B **152**, 22 (1988).
[21] M. Y. Choi and D. Stroud, Phys. Rev. B **35**, 7109 (1987); M. Y. Choi, J. S. Chung, D. Stroud, and J. Choi, *ibid.* **40**, 5147 (1989).
[22] T. C. Halsey, Phys. Rev. B **31**, 5728 (1985).
[23] C. Denniston and C. Tang, e-print cond-mat/9710060; see also P. Gupta, S. Teitel, and M. J. P. Gingras, Phys. Rev. Lett. **80**, 105 (1997).
[24] K. Binder and A. P. Young, Rev. Mod. Phys. **58**, 801 (1986); K. H. Fischer and J. A. Hertz, *Spin Glasses* (Cambridge University Press, Cambridge, 1991); *Spin Glasses and Random Fields*, edited by A. P. Young (World Scientific, Singapore, 1998).
[25] L. J. Lewis and G. Wahnström, Phys. Rev. E **50**, 3865 (1994); G. Wahnström and L. J. Lewis, Prog. Theor. Phys. Suppl. **126**, 261 (1997).
[26] F. Sciortino, P. Gallo, P. Tartaglia, and S.-H. Chen, Phys. Rev. E **54**, 6331 (1996).
[27] S. Kämmerer, W. Kob, and R. Schilling, Phys. Rev. E **56**, 5450 (1997).
[28] D. Sidebottom, R. Bergman, L. Börjesson, and L. M. Torell, Phys. Rev. Lett. **68**, 3587 (1992); **71**, 2260 (1993).
[29] W. Götze and L. Sjögren, Rep. Prog. Phys. **55**, 241 (1992).
[30] N. Menon and S. R. Nagel, Phys. Rev. Lett. **74**, 1230 (1995); R. L. Leheny and S. R. Nagel, Europhys. Lett. **39**, 447 (1997).
[31] P. Lunkenheimer, A. Pimenov, M. Dressel, Yu. G. Goncharov, R. Böhmer, and A. Loidl, Phys. Rev. Lett. **77**, 318 (1996).
[32] D. Bitko, N. Menon, S. R. Nagel, T. F. Rosenbaum, and G. Aeppli, Europhys. Lett. **33**, 489 (1996).
[33] B. Kim and G. F. Mazenko, Phys. Rev. A **45**, 2393 (1992).
[34] H. Miyagawa, Y. Hiwatari, B. Bernu, and J. P. Hansen, J. Chem. Phys. **88**, 3879 (1988).
[35] G. Wahnström, Phys. Rev. A **44**, 3752 (1991).
[36] S. Sanyal and A. K. Sood, Europhys. Lett. **34**, 361 (1996); Prog. Theor. Phys. Suppl. **126**, 163 (1997).
[37] S. Sastry, P. G. Debenedetti, and F. H. Stillinger, Nature (London) **393**, 554 (1998); see also A. Angell, *ibid.* **393**, 521 (1998).
[38] F. Fujara, B. Geil, H. Sillescu, and G. Fleischer, Z. Phys. B **88**, 195 (1992); M. T. Ciceron and M. D. Ediger, J. Chem. Phys. **104**, 7210 (1996), and references therein.
[39] D. N. Perera and P. Harrowell, Phys. Rev. Lett. **81**, 120 (1998).
[40] R. Yamamoto and A. Onuki, Phys. Rev. E **58**, 3515 (1998).
[41] M. Nicodemi and A. Coniglio, Phys. Rev. E **57**, R39 (1998).
[42] S. J. Lee and B. Kim, and J.-R. Lee, e-print cond-mat/9810149.
[43] R. D. Mountain and D. Thirumalai, Phys. Rev. A **36**, 3300 (1987).
[44] A. Rahman, Phys. Rev. A **136**, A405 (1964).
[45] T. Odagaki and Y. Hiwatari, Phys. Rev. A **43**, 1103 (1991).
[46] W. Kob and H. C. Andersen, Phys. Rev. E **51**, 4626 (1995).
[47] M. M. Hurley and P. Harrowell, J. Chem. Phys. **105**, 10 521 (1996).
[48] J.-N. Roux, in *Slow Dynamics in Condensed Matter*, Proceedings of The First Tohwa University International Symposium, edited by K. Kawasaki, T. Kawakatsu, and M. Tokuyama (AIP, New York, 1991); H. Löwen, J.-P. Hansen, and J.-N. Roux, Phys. Rev. A **44**, 1169 (1991).
[49] T. Gleim, W. Kob, and K. Binder, Phys. Rev. Lett. **81**, 4404 (1998).